International Journal of Power Electronics and Drive System (IJPEDS)
Vol. 17, No. 1, March 2026, pp. 238~249
ISSN: 2088-8694, DOI: 10.11591/ijpeds.v17.i1.pp238-249

Performance of high-speed train traction motor system in acceleration – cruise mode: theoretical analysis

Tri Widodo[1], Syamsul Kamar[1], Hilda Luthfiyah[1], Eko Syamsuddin Hasrito[1], Sofwan Hidayat[1], Meiyanne Lestari[1], Heru Basuki[2]
[1]Research Center for Transportation Technology, National Research Innovation and Technology, South Tangerang, Indonesia
[2]Research Center for Behavioral and Circular Economy, National Research Innovation and Technology, South Tangerang, Indonesia

Article Info

Article history:

Received Mar 27, 2025
Revised Feb 6, 2026
Accepted Feb 15, 2026

Keywords:

Acceleration mode
Cruise mode
High speed train
Performance of traction motor
Traction motor system

ABSTRACT

This research is based on the development of a 480-kW traction motor for high-speed train (HST) applications. The performance of the traction motor system will be reviewed theoretically with the focus of the research on operational modes, namely acceleration mode and cruise mode. Motor performance will be reviewed more in-depth related to the development of mathematical models for torque function of time, power function of time and efficiency function of speed. The data used in this study are real data of 480 kW traction motor specifications and synthetic data of HST operations. The results of the traction motor performance analysis show that in the operational conditions of acceleration mode, the traction motor requires power and torque at the beginning reaching 4,838.13 Nm to overcome inertia, friction, aerodynamic force and increase speed. In cruise mode, the speed tends to be stable, so the power and torque decrease to 1,133.24 Nm. The results of the traction motor performance theoretically show that the traction motor can work well for variations in speed and track profile.

Corresponding Author:

Hilda Luthfiyah
Research Center for Transportation Technology, National Research and Innovation Agency
KST B.J. Habibie BRIN Serpong, South Tangerang, Banten 15314, Indonesia
Email: hilda.luthfiyah@brin.go.id

1. INTRODUCTION

High-speed rail (HST) systems are designed to provide fast, reliable and comfortable transportation, and can significantly reduce travel time between major cities [1], [2]. HST is known to be more efficient in energy use than other air and land transportation over the same distance [3]. In HST, the traction transmission system converts electrical energy supplied from the electricity grid into mechanical energy for train movement by transferring torque, thus providing a stable power source for the train [4]. The power requirements of HST mainly include energy for the traction system and some for auxiliary facilities. The auxiliary energy is generally constant, while the traction energy will vary over time, because it is determined by the operating conditions of the train such as acceleration, when traveling at a constant speed, and when braking when approaching a station. In addition, the railway track profile such as the rate of ascent and descent, radius of curvature, and rolling resistance, as well as the weight of the train also affect the power requirements of the HST traction motor system [5]. Aerodynamics plays an important role in the energy efficiency, stability, and comfort of HST, especially when traveling at very high speeds. At high speeds, aerodynamic forces such as drag (air resistance) and lift (lifting force) become critical factors that affect the energy efficiency and stability of the train [6].

Currently, HST generally uses electrical multiple units (EMU) to meet energy consumption to be more efficient while providing optimal traction and braking performance. Figure 1 shows the layout of the

HST used as a model in this study. The traction drive system in HST with EMU involves complex interactions between electrical components such as traction motors, inverters, and control systems with mechanical components such as gearboxes and wheels [7]. Several studies have been developed to reduce energy consumption in trains through energy evaluation of the train traction drive system [8], management of the traction power supply system [9], electromechanical clutch models [4], combining mechanical-electrical-hydraulic dynamic clutch drive systems (MEH-DCDS) [10], and through traction transmission system control (TTS) [11]. This control technology has also been developed using the model predictive control (MPC), adaptive control, and sliding mode control (SMC) methods [12].

Various studies on the design and performance analysis of traction motors in urban trains, HST, and maglev trains have been conducted, including Hamedani *et al.* [13] build a simulation of the mechanical movement of DC electric trains in the form of a regenerative braking model and steering control with coasting control. Then the optimization model of the urban train travel curve in fast and slow train modes has also been created [14]. The simulation calculation of the maglev train traction is designed and the simulation system is developed using the actual operational train track [15]. In addition, research on driving strategy optimization and field test results on the urban rail transportation system has been carried out [16] as well as an analysis of the efficiency of 180 kW motors on urban trains [17].

In Indonesia, there has been a rapid increase in electric-based train drive system technology. Urban trains use traction motors with an output power of 100 kW and 180 kW [18], [19]. Then there is a type of diesel electric multiple unit (DEMU) that uses a traction motor with an output power of 550 kW [20]. In addition, the HST route Jakarta-Bandung is currently operating with a maximum operating speed of 350 km/h [21]. As a comparison, HST in the world which has a speed of 250-300 km/h generally uses traction motors with specifications between 300-1200 kW [12], [22], [23]. In Indonesia itself, the HST route Jakarta-Surabaya is currently being developed with a speed of 250-300 km/h. To be able to achieve this speed, a squirrel cage induction motor (SCIM) design has been developed for the 480 kW EMU [24]. However, the 480-kW motor design has not simulated the traction motor system, which is affected by the train's operational travel mode, namely during acceleration mode and cruise mode.

Most previous studies have primarily focused on total energy consumption and power control strategies. However, limited research has been conducted on the detailed fragmentation of operational modes (i.e., acceleration and cruising) and the modeling of resistive forces including inertia, aerodynamic drag, and gradient resistance within a simplified mathematical framework. Such a framework would facilitate integration with drive train simulations and real-time control platforms, particularly for 480 kW traction motors. This study seeks to address these gaps by proposing a model that balances computational efficiency and analytical accuracy for the early-stage performance evaluation of traction motors.

We present a simulation of a 480-kW high-speed train traction motor operating under two main conditions—acceleration and cruising based on theoretical analysis. The analysis includes an examination of the motor’s torque dynamics, power consumption, and operational efficiency under various conditions, as well as an assessment of how speed variations and track profiles influence power requirements. Although this study focuses on the modeling of the traction motor, the overall performance of a high-speed train is highly dependent on the integration of the motor with the inverter, power converter, and control strategy. Therefore, future research should be directed toward investigating the motor–inverter interface to optimize energy consumption, enhance efficiency, and enable the integration of regenerative energy recovery systems.

Figure 1. HST layout

2. HST TRAVEL OPERATIONAL MODE

The calculation of train movement is based on Newton's laws of motion, considering gradients, speed limitations, and operating modes [25]. In this study, the performance of the traction motor system is focused on the acceleration and cruise modes.

2.1. Acceleration ode

Acceleration mode is a mode in which the train quickly increases its speed from a standstill or initial speed to cruise speed. When acceleration mode occurs, HST requires high torque at the start of acceleration to overcome inertia and accelerate the train. As a result, power consumption reaches a maximum because the motor works harder to provide acceleration. The total HST force that arises in this mode is aerodynamic force, wheel friction, incline resistance, and acceleration force. Acceleration mode has a short duration because the

train is only in this mode until it reaches cruise speed. In this study, the speed of HST acceleration mode is limited from 0 km/h to 0.9×v_{max}. If the maximum speed (v_{max}) is 55.5 m/s, then the speed limit is 0-50 m/s.

2.1.1. Cruise mode

Cruise mode occurs when the train has reached a constant speed and no longer experiences significant acceleration or deceleration. The power in the traction motor is used to overcome air resistance and friction. Cruise mode has lower torque than acceleration mode because the motor only needs to maintain speed. This affects the power consumption in the HST which is lower than in acceleration mode because no additional energy is needed to increase speed. The total force in cruise mode comes from aerodynamic forces, wheel friction, and uphill resistance (no acceleration force). However, the duration of cruise mode is longer than acceleration mode because the train can remain in this mode for a long distance. In this study, the speed of cruise mode is limited from 0.9×v_{max} to v_{max}, so the speed limit is 50 - 55.5 m/s. A comparison of these two modes can be seen in Table 1.

Table 1. Characteristics of acceleration mode and cruise mode

Parameter	Acceleration mode	Cruise mode
Speed	Increase (v↑)	Constant (v fixed)
Acceleration (a)	$a > 0$	$a \approx 0$ (approaches 0)
Motor torque	Tall	Lower
The style at work	Inertia, aerodynamics, friction, slope	Aerodynamics, friction, ramp
Duration	Short	Long

3. METHODOLOGY

3.1. HST traction motor specifications

Based on performance requirements and field conditions, the general technical specifications of traction motors for HST can be seen in Table 2. The design specifications of traction motors in Table 2 are sourced from similar studies and input from traction motor engineering experts. Several factors considered in designing traction motors are that the motor must have efficiency and power factor in accordance with high initial torque requirements. Table 3 contains data on similar HST facilities with the same or similar specifications to the HST that we designed and have been developed in other studies or have been built in the railway industry. This data is used to determine the performance of traction motors during HST operational conditions, namely when acceleration mode and cruise mode are required.

Table 2. HST traction motor specifications

Parameter	Type/value
Motor power (P)	480 kW
Voltage (V)	2300 VAC
Frequency (f)	85 Hz
Speed (N)	1500 rpm
Efficiency (η)	95%
Wheel Spokes	0.5 m

Table 3. Synthetic parameters for HST in development

Parameter	Value
Number of train sets	4 series
Total mass of train (m)	400,000 kg
Air resistance coefficient (C_d)	0.2 – 0.3
Frontal cross-sectional area (A)	10 – 12 m²
Maximum rail gradient (θ)	4°
Coefficient of friction (f_r)	0.002 – 0.005
Gear ratio (GR)	3
Air density (ρ)	~1.225 kg/m ^{3}
Gravity (g)	9.81 m/s ^{2}

3.2. Mathematical modeling

3.2.1. Calculation of the forces acting on the HST

The forces acting on HST start from Newton's force (F_{acc}) in (1).

$$F_{acc} = m\ x\ a \quad (1)$$

Then the aerodynamic drag force (F_{aero}) appears, in (2).

$$F_{aero} = \frac{\rho \, x \, C_d \, x \, A \, x \, v^2}{2} \quad (2)$$

In addition, in the HST, there is also a frictional resistance force ($F_{rolling}$) according to (3).

$$F_{rolling} = f_r \, x \, m \, x \, g \quad (3)$$

When the HST operates on an uphill road ($\theta > 0$), an uphill resistance force (F_{grade}) appears as shown in (4).

$$F_{grade} = m \, x \, g \, x \, \sin\theta \quad (4)$$

So, the total force that must be compensated by the traction motor in (5).

$$F_{total} = F_{acc} + F_{drag} + F_{rolling} + F_{grade} \quad (5)$$

The traction motor torque value occurs based on the relationship between the total force acting on the train and the radius of the train wheels. The (6) shows the relationship between the traction motor torque and the force acting on the train, as in (6).

$$T_m = \frac{F_{total} \, x \, r_{wheel}}{\eta} \quad (6)$$

Where T_m is the motor torque, F_{total} is the total force (N), r_{wheel} is the radius of the train wheel.

3.2.2. Traction motor power consumption

Consumption on HST during acceleration mode is certainly different from HST in cruise mode. When HST is in acceleration mode, the torque that works is greater when compared to cruise mode. The motor power consumption equation is as seen in (7).

$$P_{motor} = \frac{T_m \, x \, \omega}{\eta} \quad (7)$$

Where P_{motor} is the motor power (watts), ω is the angular velocity (rad/s). Then the angular velocity of the motor is found as shown in (8).

$$\omega = \frac{2 \, x \, \pi \, x \, N}{60} \quad (8)$$

Where N is the number of revolutions (rpm).

3.2.3. Analyzing the efficiency comparison of acceleration and cruise modes

In the actual system, the electrical power input to the motor is obtained from a DC–AC converter-based inverter. The inverter efficiency η_{inv} and the control strategy (V/f) will affect the input power value P_{in} in (10). Thus, the total efficiency of the drive system can be defined as (9).

$$\eta_{system} = \eta_{inv} \, x \, \eta_{motor} \quad (9)$$

The efficiency of the HST traction motor is calculated using (10).

$$\eta_{operational} = \frac{P_{out}}{P_{in}} \, x \, 100\% \quad (10)$$

Where P_{outt} is output power, P_{in} is input power.

3.3. Traction motor performance analysis

3.3.1. The relationship between motor torque and time function

In an HST drive system, traction motor torque is the main factor that determines how the acceleration and speed of the train develop over time. Motor torque as a function of time describes how the force produced by the motor changes in various stages of train operation, from acceleration, cruise, to deceleration. The torque (T_m) produced by the electric motor can be described as a function of time using (11).

$$T_m = \frac{m \, x \, \frac{dV(t)}{dt} \, x \, r}{GR} \quad (11)$$

Where *GR* is the Gear Ratio, *V(t)* is the speed at time t.

3.3.2. The relationship between power and time function

In high-speed rail systems, power as a function of time plays a major role in understanding the efficiency and performance of train operation in acceleration mode and cruise mode. The (12) shows the total power output by the motor, and (13) shows the total force appearing in the motor affected by time.

$$P(t) = F(t)\ x\ v(t) \tag{12}$$

$$F(t) = m.a(t) + F_{rolling} + F_{aero} \tag{13}$$

Where *P(t)* is the total power function of time, is *F(t)* is the total force function of time. The higher the speed, the greater the power required because the aerodynamic drag increases exponentially in (14).

$$F_{aero} \propto v^2 \tag{14}$$

3.3.3. Relationship between efficiency and speed function

In HST transportation systems, energy efficiency as a function of speed plays an important role in optimizing performance and power consumption. This efficiency depends on the operating speed, external drag force, and traction motor characteristics. The relationship between efficiency (η) and speed (v) is based on the principles of electric vehicle physics and engineering in (15).

$$\eta = \frac{P_{out}}{P_{in}} \tag{15}$$

Where P_{out} is the mechanical power used to drive the train, P_{in} is the electrical power supplied to the traction motor from the electrical system, η is the Efficiency of the motor varies depending on the resistance factor which changes with speed.

In addition to numerical analysis, simulation results are visualized graphically to facilitate trend interpretation. Included plots include torque versus time, power versus time, power versus speed, and efficiency versus speed. These graphs are used to identify critical operating points and peak motor demand, and to apply these to motor sizing, cooling systems, and energy management.

3.4. Sensitivity and uncertainty analysis

3.4.1. Local sensitivity analysis

Local sensitivity analysis is conducted to assess the effect of small changes in input parameters on model output, specifically traction motor torque. This approach uses a numerical differentiation method (finite difference method) around the nominal parameter values [26]. Parameter changes are made one at a time with variations of ± Δy and ± Δp, while other parameters are kept constant. The sensitivity coefficient is calculated as a normalized sensitivity in (16).

$$S_p = \left(\frac{\Delta y}{y}\right) / \left(\frac{\Delta p}{p}\right) \tag{16}$$

Where S_p indicates the relative rate of change in output (y) relative to the relative change in parameter (p).

The parameters analyzed include the track gradient (θ), the rolling coefficient (f_r), and the drag coefficient (C_d). This analysis provides an initial understanding of the system's sensitivity around the nominal operating point and serves as a basis for determining the parameter variation range for the global sensitivity analysis.

3.4.2. Sensitivity analysis and global uncertainty

A global sensitivity analysis is used to evaluate the simultaneous influence of all parameters on model output, as well as the interactions between parameters. The approach used is monte Carlo sampling (MCS) with a sample size of N=5,000 [27]. Five main parameters are used as random variables: trajectory gradient (θ), rolling coefficient (f_r), drag coefficient (C_d), total mass (m), and frontal area (A). Parameters with fixed value boundaries are assumed to have a uniform distribution, while parameters with natural variation around their nominal values are assumed to be normal. At each iteration, a set of parameters is randomly drawn from a predetermined distribution to calculate model outputs (torque, power, efficiency). This process is repeated thousands of times to form a statistical distribution of the results. The mean, standard deviation, median, and 5–95% confidence interval is calculated to describe model uncertainty.

To assess the relationship between input and output parameters, the partial rank correlation coefficient (PRCC) is used, which calculates the partial correlation between variables while controlling for the influence of other parameters. PRCC values range from −1 to +1, with larger absolute values indicating a parameter's greater influence on model output variation. The PRCC method is effective for identifying global sensitivity in nonlinear systems and has been widely applied in uncertainty studies [28]. The combination of the MCS and PRCC approaches allows for a more comprehensive sensitivity analysis than simple deterministic methods. Simulations were conducted using Python 3.8.

In addition to sensitivity, real-world limitations must be considered. Motor traction performance is limited by winding temperature and cooling capacity, so the continuous torque rating is lower than the theoretical peak torque. Similarly, inverter dynamics (switching losses, current harmonics) can reduce system efficiency by several percent compared to ideal estimates. These factors must be taken into account during design, particularly for long-term operation and high-gradient track conditions.

4. TEST RESULTS AND ANALYSIS

Based on the traction motor specification data in Table 2 and the description of the HST operational conditions in Table 3, an analysis of the total force, HST traction motor torque, and HST traction motor power consumption that occurs on the HST in acceleration mode and cruise mode is carried out, which can be seen in Table 4. Table 4 shows that the speed gradually increases linearly with increasing time. Conversely, the increasing speed then at a certain point the acceleration decreases until it approaches zero. From the table shows the acceleration mode starting from still moving to a speed approaching 50 m/s, in cruise mode the speed has started to stabilize starting from a speed of 50 m/s to 55 m/s. In HST operations, speed as a function of time as seen in Figure 2.

Table 4. Calculation of force, torque and power of HST traction motor

t (s)	V (m/s)	a (m/s²)	F (N)	T_m (Nm)	P (W)
1	1.37	2.71	541,870.89	4,838.13	46,503.95
10	21.02	1.73	345,356.53	3,083.54	453,809.08
20	34.62	1.05	209,364.51	1,869.33	453,060.04
30	42.87	0.63	126,922.45	1,133.24	340,055.46
40	47.87	0.38	76,943.84	687.00	230,185.42
50	50.90	0.23	46,645.45	416.48	148,377.63
60	52.73	0.14	28,277.74	252.48	93,196.77
70	53.85	0.09	17,142.73	153.06	57,691.44
80	54.52	0.05	10,392.39	92.79	35,412.57
90	54.93	0.03	6,300.15	56.25	21,629.19
100	55.18	0.02	3,819.32	34.10	13,171.42

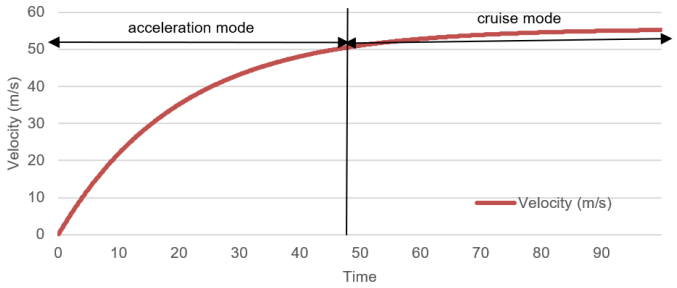

Figure 2. HST operational speed with time function variation

4.1. Relationship between motor torque and time function

The torque with a function of time produced by the traction motor is affected by the train's operating mode, namely acceleration mode and cruise mode. Figure 3(a) shows the performance of the traction motor versus the function of time based on the data in Table 4. In acceleration mode, there is an increase in torque at the beginning of time. This is because the traction motor must provide a large thrust to overcome the train's inertia, wheel friction, aerodynamic force and increased speed. If the acceleration remains constant, the torque remains at a high value before starting to decrease as the speed increases. In cruise mode, after the speed is stable, the acceleration approaches zero ($a \approx 0$) then the torque tends to decrease and tends to stabilize at a lower value. Torque is used to counteract resistance such as wheel friction, air resistance, and

track profile. The torque in cruise mode is constant and lower than in acceleration mode, because it functions to maintain speed.

Furthermore, the initial torque (≈4,838 Nm) is observed during acceleration, which then decreases and stabilizes at around 1,100 Nm in cruise mode. This underscores the importance of designing a motor with high initial torque capability to overcome the inertia and resistive forces of the HST. The motor performance described here is closely related to the converter control strategy. The use of field-oriented control (FOC) or model predictive control (MPC) can maintain optimal torque while minimizing switching losses. Furthermore, the integration of regenerative braking allows energy recovery on downhill slopes, thus reducing total energy consumption. The developed model can be interfaced with the control system to transmit motor responses in real-time scenarios.

4.2. The relationship between power and time function

The power consumed by the traction motor is highly dependent on the speed and torque produced. Power in the function of time in this study is useful for knowing the amount of power consumption issued at each time change in order to predict the performance of the traction motor being developed. In its implementation, power on the HST occurs when the characteristics of acceleration mode and cruise mode. Figure 3(b) shows that in acceleration mode there is a power surge at the beginning of time because the traction motor requires large power to overcome vehicle inertia, frictional resistance, aerodynamic resistance based on Table 4. It can be seen in the acceleration mode phase that if the acceleration is high, the power will jump sharply and last for a short time, while if the acceleration is low, the power will increase gradually and last longer. In this mode, the HST traction motor requires high power to accelerate the train quickly. Power consumption increases with vehicle inertia, track profile, and air resistance. When in cruise mode, power consumption tends to be stable. This is because the motor only needs to overcome aerodynamic resistance and frictional resistance, without the need to increase speed further. When the HST cruising speed is low to medium, power consumption is relatively small and stable. This is because no energy is used to increase speed. Meanwhile, if the HST cruising speed is high, power consumption is greater because aerodynamic resistance increases. After the power reaches its peak, then the power begins to stabilize or begins to decrease because the acceleration decreases. Energy consumption tends to increase with speed due to the effect of aerodynamic resistance.

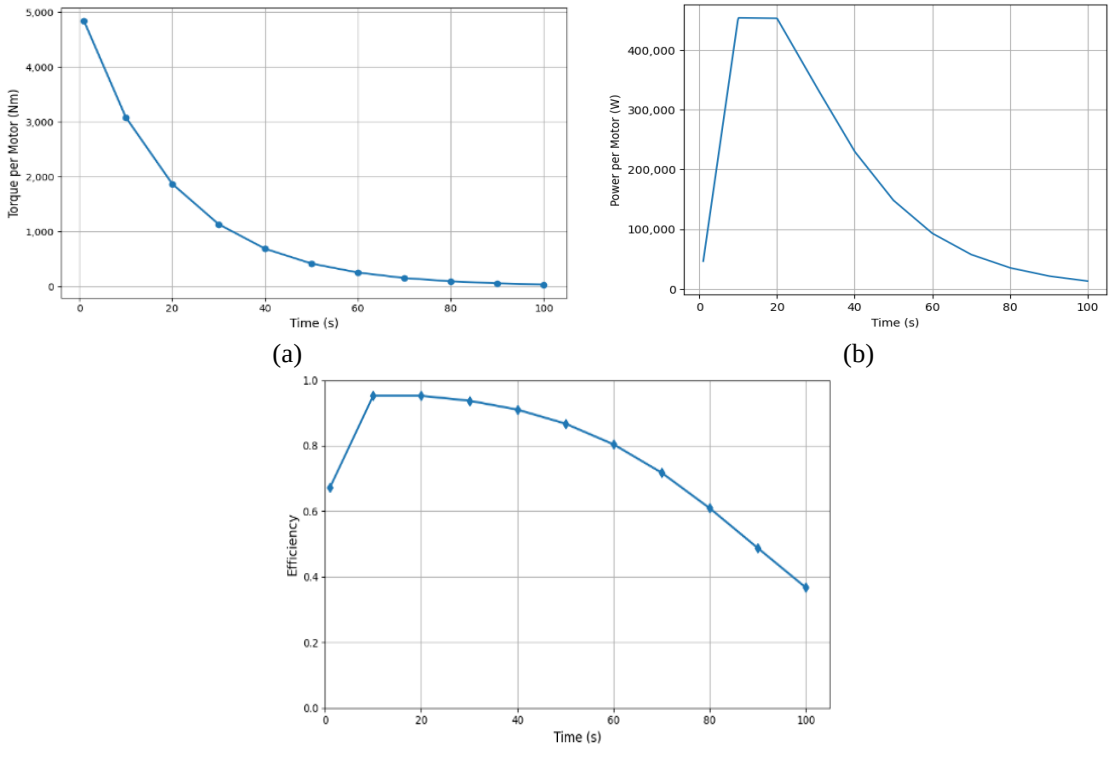

Figure 3. Dynamic performance characteristics of the traction motor: (a) torque motor - time function, (b) power motor – time function, and (c) efficiency motor – time function

4.3. Relationship between efficiency and speed

Efficiency (η) in the HST propulsion system describes how effectively the energy used to generate traction power is compared to the total energy consumed from the power source. This efficiency varies as a function of time due to changes in operational mode, traction force, and the influence of aerodynamic drag and wheel friction on the rail. Figure 3(c) is a graph of the relationship between motor efficiency and HST speed based on the data in Table 4, also can be seen that efficiency (η) changes non-linearly with speed (v). When the acceleration mode is low, the efficiency of the HST traction motor is low when the train starts moving up to a speed of 13.89 m/s because at the beginning the inertia factor affects it to overcome the initial resistance force. The value of electrical losses in the motor is high due to the large current at high initial torque. This energy is mostly used for acceleration rather than to maintain speed. Efficiency increases with increasing speed.

Then in cruising mode at medium speed (13.9 m/s – 33.3 m/s) efficiency continues to increase with increasing speed because the traction motor gradually works more optimally where power losses are minimal and the energy produced is greater. At high speeds (33.4 m/s–55.5 km/h) aerodynamic losses increase so that the motor works to maintain speed. In addition, electrical losses from the traction motor also increase significantly resulting in decreased efficiency. Low energy losses, because the motor works at the highest efficiency range (~85%-95%), and minimal power conversion losses and optimal motor torque, but there is exponentially increasing aerodynamic resistance ($F_{aero} \propto v^2$), requiring more power. When the HST traction motor starts to exit the optimal efficiency range, it causes electrical losses to increase. The effect is that the internal resistance of the transmission system and friction increase. At near maximum speed (v_{max}) the input power increases much faster than the output power, causing a drastic drop in efficiency due to aerodynamic and electrical losses. This trend indicates that the most efficient operation is achieved in the mid-speed range. It should be noted that the theoretical efficiency obtained in a motor may differ from actual conditions, because the inverter system adds switching losses and harmonics. Inverter control strategies such as PWM or MPC can be used to suppress these losses and increase energy recovery through regenerative braking.

4.4. Relationship between speed variations and path profile affecting torque and power requirements

The power requirement of the traction motor is affected by the train speed and the track profile. Figure 4 shows the power versus speed characteristics, where peak power consumption exceeds 450 kW at medium speeds (20–35 m/s) before stabilizing at approximately 150–200 kW during cruising conditions. At low speeds, the power consumption is greater because the motor efficiency is lower and requires large torque. At medium speeds (30-50 m/s), the power consumption begins to stabilize because the efficiency increases. This pattern indicates that traction motor sizing should not be based solely on maximum speed conditions, but must also consider the significant power demand occurring at medium-speed operation.

The effect of the road profile, especially on flat tracks ($\theta = 0$), then the power is used for aerodynamic resistance and friction. While if the track is uphill ($\theta > 0$) results in additional force F_{grade} appearing, so that the power increases. When the track is downhill ($\theta < 0$), the motor can operate in regenerative mode, converting kinetic energy into electricity. Further analysis shows that when the track gradient increases from 2° to 4°, the torque requirement increases significantly by ~15 – 20% compared to flat tracks. This condition causes the motor to work harder and increases power consumption, especially during the acceleration phase. Conversely, on downhill tracks, the motor can operate in regenerative mode, resulting in reduced power consumption and energy recovery opportunities. Motor loading due to variations in train mass (e.g., ± 10% of total weight) also has an impact on increasing the initial torque requirement and shifting the operating efficiency point. This shows that track gradient and train load are important parameters that affect motor performance.

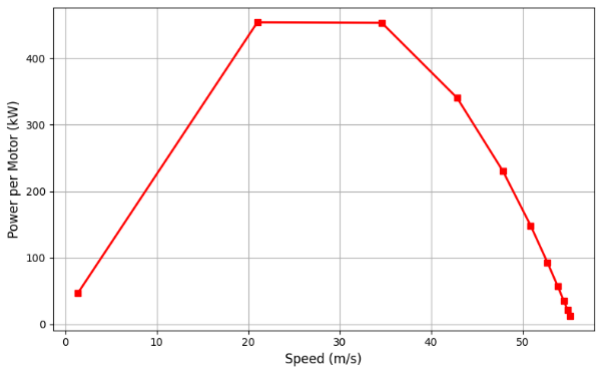

Figure 4. Power as a function of speed

4.5. Sensitivity results

The results of the local sensitivity analysis indicate that track gradient (θ) is the most dominant factor influencing traction motor torque requirements. Every 1° (≈ 0.017 rad) increase in track angle causes an increase in T_m of approximately 713.4 Nm per motor, or approximately 62.9% of the baseline torque value under cruise conditions. This indicates that small changes in road gradient have a significant impact on motor load. Conversely, a 0.001 increase in f_r only increases torque by approximately 40.9 Nm, or 3.6% of the baseline, while a 0.05 increase in C_d only adds approximately 6.5 Nm, or 0.6% of the baseline. This comparison clarifies that aerodynamic resistance and friction contribute relatively little to the influence of gradient.

A global sensitivity analysis was performed using MCS with 5,000 iterations to evaluate the simultaneous influence of all parameters on torque variation. Simulation results indicate that the median T_m under cruise conditions is approximately 1,585.9 Nm per motor, with a 5–95% confidence interval of 319.1–2,897.0 Nm, or approximately ±82.7% of the median value. This relatively wide range of variation indicates that uncertainty in the input parameters significantly influences the distribution of output torque, particularly due to changes in gradient and total mass. This variability indicates that the traction system is highly sensitive to external conditions such as track gradient and train load.

The results of the partial correlation analysis using Spearman rank correlation (as a PRCC approach) show that $\theta = 0.994$, the highest correlation coefficient. It is indicates θ has a very strong positive relationship with T_m. This means that the greater the path gradient, the higher the torque required to maintain speed. The m has a moderate positive correlation of 0.105, while f_r and C_d show low correlation values of 0.040 and −0.011, respectively. The A has almost no effect with a value of −0.002.

4.6. Discussion

The implications of the simulation results indicate that traction motor design needs to account for high starting torque capacity to handle transient loads during the acceleration phase. This requires adjustments to the motor diameter, gear ratio, and inverter current rating to ensure the system can deliver peak torque consistently without performance degradation. Furthermore, the increase in peak power consumption during the acceleration phase indicates the need for an efficient cooling system to prevent excessive winding temperature rise (overheating). Implementing a liquid-based active cooling system or transient-based dynamic thermal management could be effective solutions for maintaining stable operating temperatures.

From an energy management perspective, integration with a regenerative braking strategy has the potential to balance energy consumption and improve overall efficiency, particularly under track conditions with varying gradients and dynamic speed patterns. Although this research focuses on modeling traction motor performance, the overall performance of an HST traction system is highly dependent on the integration of the motor, inverter, power converter, and control strategy. Therefore, further research could be directed at developing a motor-inverter co-simulation model to optimize energy efficiency, improve dynamic performance, and implement a regenerative energy recovery system.

5. CONCLUSION

This study models and analyzes the performance of traction motors on high-speed trains (HST) under two main operating conditions: acceleration and cruising. Simulation results show that during the initial acceleration phase, the motor requires up to ±453 kW of power and a peak torque of ±4,838 Nm to overcome inertial forces, friction, and aerodynamic drag. After the speed stabilizes (>30 s), the torque decreases to approximately 1,133 Nm, with peak efficiency at moderate speeds (~40–160 km/h). This emphasizes the importance of torque control and power management during the acceleration phase to maintain energy efficiency. Practical implications of this study include identifying the efficient operating point, providing a basis for selecting motor size and cooling capacity, and supporting inverter control and energy regeneration strategies. This model also has the potential to be developed for multi-motor configurations and motor-inverter integration to improve the efficiency of electric traction systems in modern rail transportation applications.

This study has several limitations that require attention. First, the developed model still assumes ideal conditions, namely a constant gear ratio, no wheel slippage, and constant motor efficiency. Second, experimental validation or real-time simulation have not been conducted, so the results obtained are still conceptual and require further verification. Third, the scope of the study does not include comparisons with other motor traction models or widely used inverter control strategies, such as field-oriented control (FOC), MPC, and direct torque control (DTC). Furthermore, although sensitivity and uncertainty analyses are included, this model does not consider nonlinear dynamics that can arise from wheel slippage or creep, variations in inverter losses, or the influence of sophisticated control systems. For future research, this model

can be developed through integration with the motor-inverter system and tested on a real-time simulation platform to obtain more representative dynamic performance validation. Further studies are also recommended to incorporate more complex gradient variations, coefficient degradation due to weather conditions, and changes in dynamic aerodynamic profiles to further align the model with actual operational conditions on real-world tracks.

FUNDING INFORMATION

Authors state no funding involved.

AUTHOR CONTRIBUTIONS STATEMENT

This journal uses the Contributor Roles Taxonomy (CRediT) to recognize individual author contributions, reduce authorship disputes, and facilitate collaboration.

Name of Author	C	M	So	Va	Fo	I	R	D	O	E	Vi	Su	P	Fu
Tri Widodo	✓	✓	✓		✓	✓	✓	✓	✓	✓	✓		✓	
Syamsul Kamar	✓	✓		✓	✓		✓		✓	✓		✓		✓
Hilda Luthfiyah		✓	✓		✓	✓	✓	✓	✓	✓	✓		✓	
Eko Syamsuddin Hasrito	✓		✓			✓		✓	✓	✓	✓		✓	
Sofwan Hidayat	✓		✓	✓	✓			✓		✓		✓		✓
Meiyanne Lestari		✓		✓		✓				✓		✓	✓	✓
Heru Basuki		✓				✓	✓			✓	✓	✓		

C : **C**onceptualization
M : **M**ethodology
So : **So**ftware
Va : **Va**lidation
Fo : **Fo**rmal analysis
I : **I**nvestigation
R : **R**esources
D : **D**ata Curation
O : Writing - **O**riginal Draft
E : Writing - Review & **E**diting
Vi : **Vi**sualization
Su : **Su**pervision
P : **P**roject administration
Fu : **Fu**nding acquisition

CONFLICT OF INTEREST STATEMENT

Authors state no conflict of interest.

DATA AVAILABILITY

The data that support the findings of this study are available on request from the corresponding author, [TW]. The data, which contain information that could compromise the privacy of research participants, are not publicly available due to certain restrictions.

REFERENCES

[1] P. Chenrrim and S. Relvas, "A data envelopment analysis approach for evaluating high-speed freight transportation efficiency," *Transportation Research Interdisciplinary Perspectives*, vol. 29, 2025, doi: 10.1016/j.trip.2025.101338.
[2] S. Xu, C. Chen, Z. Lin, X. Zhang, J. Dai, and L. Liu, "Review and prospect of maintenance technology for traction system of high-speed train," *Transportation Safety and Environment*, vol. 3, no. 3, 2021, doi: 10.1093/tse/tdab017.
[3] I. Watson, A. Ali, and A. Bayyati, "Energy efficiency of high-speed railways," *Advances in Environmental and Engineering Research*, vol. 3, no. 4, 2022, doi: 10.21926/aeer.2204055.
[4] K. Zhang, J. Yang, C. Liu, J. Wang, and D. Yao, "Dynamic characteristics of a traction drive system in high-speed train based on electromechanical coupling modeling under variable conditions," *Energies*, vol. 15, no. 3, 2022, doi: 10.3390/en15031202.
[5] A. M. Elagab and I. M. El-Amin, "The impact of electrical traction drives on power system quality under different loading conditions," *Arabian Journal for Science and Engineering*, vol. 47, no. 11, pp. 14695–14710, 2022, doi: 10.1007/s13369-022-06774-w.
[6] D. Weidner, D. Stoll, T. Kuthada, and A. Wagner, "Aerodynamics of high-speed trains with respect to ground simulation," *Fluids*, vol. 7, no. 7, 2022, doi: 10.3390/fluids7070228.
[7] I. A. Tasiu, Z. Liu, S. Wu, W. Yu, M. Al-Barashi, and J. O. Ojo, "Review of recent control strategies for the traction converters in high-speed train," *IEEE Transactions on Transportation Electrification*, vol. 8, no. 2, pp. 2311–2333, 2022, doi: 10.1109/TTE.2022.3140470.
[8] Z. Wu, C. Gao, and T. Tang, "An optimal train speed profile planning method for induction motor traction system," *Energies*, vol. 14, no. 16, 2021, doi: 10.3390/en14165153.
[9] H. Yang *et al.*, "Coordinated demand response of rail transit load and energy storage system considering driving comfort," *CSEE Journal of Power and Energy Systems*, vol. 6, no. 4, pp. 749–759, 2020, doi: 10.17775/CSEEJPES.2020.02590.
[10] J. Yang, T. Zhang, H. Zhang, J. Hong, and Z. Meng, "Research on the starting acceleration characteristics of a new mechanical–electric–hydraulic power coupling electric vehicle," *Energies*, vol. 13, no. 23, 2020, doi: 10.3390/en13236279.

[11] Z. Xiao, Q. Wang, P. Sun, B. You, and X. Feng, "Modeling and energy-optimal control for high-speed trains," *IEEE Transactions on Transportation Electrification*, vol. 6, no. 2, pp. 797–807, 2020, doi: 10.1109/TTE.2020.2983855.
[12] M. Torrent, J. I. Perat, and J. A. Jiménez, "Permanent magnet synchronous motor with different rotor structures for traction motor in high speed trains," *Energies*, vol. 11, no. 6, 2018, doi: 10.3390/en11061549.
[13] P. Hamedani, S. S. Fazel, and M. Shahbazi, "Modelling and Simulation of DC electric railway system with regenerative braking: A case study of isfahan metro line 1," *Journal of Electrical and Computer Engineering Innovations*, vol. 12, no. 2, pp. 439–448, 2024.
[14] L. Deng, L. Cai, G. Zhang, and S. Tang, "Energy consumption analysis of urban rail fast and slow train modes based on train running curve optimization," *Energy Reports*, vol. 11, pp. 412–422, 2024, doi: 10.1016/j.egyr.2023.12.014.
[15] H. Liu and B. Wang, "Research on traction calculation simulation system of mid-low speed maglev train," *Journal of Physics: Conference Series*, vol. 1910, no. 1, 2021, doi: 10.1088/1742-6596/1910/1/012012.
[16] N. Zhao, Z. Tian, L. Chen, C. Roberts, and S. Hillmansen, "Driving strategy optimization and field test on an urban rail transit system," *IEEE Intelligent Transportation Systems Magazine*, vol. 13, no. 3, pp. 34–44, 2021, doi: 10.1109/MITS.2019.2926369.
[17] S. Kamar *et al.*, "Performance analysis of three-phase induction motor for railway propulsion system," *International Journal of Power Electronics and Drive Systems*, vol. 14, no. 3, pp. 1433–1441, 2023, doi: 10.11591/ijpeds.v14.i3.pp1433-1441.
[18] A. Setiyoso, H. Hindersyah, A. Purwadi, and A. Rizqiawan, "Design of traction motor 180 kW type SCIM for KRL (EMU) Jabodetabek re-powering project," in *Proceedings of 2014 International Conference on Electrical Engineering and Computer Science, ICEECS 2014*, 2014, pp. 341–344, doi: 10.1109/ICEECS.2014.7045274.
[19] A. Setiyoso, K. Hadi, L. N. Mulyani, R. Sipahutar, and Y. P. P. Kesawa, "Design of traction motor 100kW for LRT rolling stock in Jabodebek – Indonesia," in *2022 7th International Conference on Electric Vehicular Technology (ICEVT)*, IEEE, Sep. 2022, pp. 153–156, doi: 10.1109/ICEVT55516.2022.9924690.
[20] A. S. Hartono, Roosdiatmoko, T. Widodo, A. Iswanto, Y. Haroen, and P. A. Dahono, "Development of new drive system of diesel electric multiple unit (DEMU) for Indonesia railway," in *Proceedings of the International Conference on Power Electronics and Drive Systems*, 2001, pp. 489–493, doi: 10.1109/peds.2001.975365.
[21] A. Purba, "The challenge of developing high-speed rail projects: recent evidence from developing countries," *International Journal of GEOMATE*, vol. 18, no. 70, pp. 99–105, 2020, doi: 10.21660/2020.70.9393.
[22] H. Zhao, J. Liang, and C. Liu, "High-speed EMUs: Characteristics of technological development and trends," *Engineering*, vol. 6, no. 3, pp. 234–244, 2020, doi: 10.1016/j.eng.2020.01.008.
[23] G. Wu *et al.*, "Pantograph–catenary electrical contact system of high-speed railways: recent progress, challenges, and outlooks," *Railway Engineering Science*, vol. 30, no. 4, pp. 437–467, 2022, doi: 10.1007/s40534-022-00281-2.
[24] H. Luthfiyah *et al.*, "An optimized stator and rotor design of squirrel cage induction motor for EMU train," *Journal of Mechatronics, Electrical Power, and Vehicular Technology*, vol. 14, no. 1, pp. 35–46, 2023, doi: 10.14203/j.mev.2023.v14.35-46.
[25] C. Sumpavakup, S. Suwannakijborihan, T. Ratniyomchai, and T. Kulworawanichpong, "Peak demand cutting strategy with an on-board energy storage system in mass rapid transit," *Iranian Journal of Science and Technology - Transactions of Electrical Engineering*, vol. 42, no. 1, pp. 49–62, 2018, doi: 10.1007/s40998-018-0048-6.
[26] G. Zhang, Q. Tong, A. Qiu, X. Xu, W. Hua, and Z. Chen, "Parameter sensitivity analysis and robust design approach for flux-switching permanent magnet machines," *Energies*, vol. 15, no. 6, 2022, doi: 10.3390/en15062194.
[27] X. Ma, Y. Zhong, P. Cao, J. Yuan, and Z. Zhang, "Uncertainty quantification and sensitivity analysis for the self-excited vibration of a spline-shafting system," *ASCE-ASME Journal of Risk and Uncertainty in Engineering Systems, Part B: Mechanical Engineering*, vol. 9, no. 4, 2023, doi: 10.1115/1.4063069.
[28] A. Pereira and R. Broed, "Methods for uncertainty and sensitivity analysis: review and recommendations for implementation in Ecolego," Stockholm Center of Physics, 2006.

BIOGRAPHIES OF AUTHORS

Tri Widodo is an engineering staff at National Research and Innovation Agency (BRIN), Indonesia. He received his Bachelor degree in electrical engineering from Brawijaya University, Malang, in 1991 and master degree in system engineering from Ibaraki University-Japan 2001. His research interest in the field of intelligent transportation system (ITS). He can be contacted at email: triw005@brin.go.id.

Syamsul Kamar is a principal engineer in Research Center for Transportation Technology (PRTT) at National Research Innovation and Technology (BRIN), Serpong, Indonesia. He received his Ir. in electrical engineering at Universitas Hasanudin in 1982, and M.T. in electrical engineering at Universitas Indonesia in 1990. His research interest includes the field of control engineering. He can be contacted at email: syamsul.kamar@brin.go.id.

Hilda Luthfiyah is an engineering staff at National Research and Innovation Agency (BRIN), Banten, Indonesia. She received her S.T. degree in physics from Sepuluh Nopember Technology Institute in 2010 and MT. degree in electrical engineering from Universitas Indonesia in 2016. Her research interest includes the field of control engineering include power electronics and system transportation. She can be contacted at email: hilda.luthfiyah@brin.go.id.

Eko Syamsuddin Hasrito is a leader of the Research Group at the National Research and Innovation Agency (BRIN). He received his B.Eng. and M.Eng. in Electronics Engineering from Ehime University, Japan, in 1994 and 1996, respectively. He received his DR.Eng. in Information Science from Chiba University, Japan, in 2001. He joined the Agency for the Assessment and Application of Technology, Indonesia, in 1988, which is currently merged into the National Research and Innovation Agency, Indonesia, for more than thirty-four years, with a focus on research on telecommunication protocols and control system design for military vehicle products and transportation system vehicles. He can be contacted at email: ekos003@brin.go.id.

Sofwan Hidayat is a principal engineer in the Research Center for Transportation Technology (PRRT), National Research Innovation and Technology (BRIN), Serpong, South Tangerang, Indonesia. He received an undergraduate engineer of Electrical Engineering from Sepuluh November Institut of Technology Surabaya (ITS) in 1987 and a Master Graduate of Electrical Engineering at Takushoku University, Tokyo, Japan in 1995. His research interests include the field of power engineering. He can be contacted at email: sofwan.hidayat@brin.go.id.

Meiyanne Lestari is an engineering staff member at the National Research and Innovation Agency (BRIN), Banten, Indonesia. She received her S.Si. degree in mathematics from Universitas Padjadjaran in 2001 and an M.T. degree in Industrial Engineering from Universitas Indonesia in 2014. She can be contacted at email: meiyanne.lestari@brin.go.id.

Heru Basuki is a principal expert engineering staff member specializing in the analysis and evaluation of engineered products resulting from Research and Technological Innovation. He has been working at the Research Center for Process and Manufacturing Technology, BRIN, Puspiptek Serpong. He earned his B.Sc. degree in 1980 and his Drs.Ec. degree in business/management from Brawijaya University, Malang, in 1983. He can be contacted at email: heru001@brin.go.id.